Bull. Fish. Sci. Hokkaido Univ.
70(1), 13–23, 2020.
DOI 10.14943/bull.fish.70.1.13

Pseudo–fortnightly variation produced by interaction between passage–flow and diurnal tidal currents in the Tsugaru Strait

Hiromi MATSUURA[1] and Yutaka ISODA[2]

(Received 11 October 2019, Accepted 28 October 2019)

Abstract

We examine the reason why non–equilibrium response of lunar fortnightly tide, i.e., Mf tide with 13.7–day period, dominates in the Japan/East Sea including the Tsugaru Strait. In the present study, tides combining with passage–flow through the (Tsugaru) Strait are numerically simulated with a two–dimensional form of hydrodynamic model. It has been known that nonlinear interaction of dominant diurnal constituents K1 and O1 results in new oscillation with the same period of Mf tide. Analysis of computed sea level and currents is aimed primarily at describing the enhanced currents and patterns of energy flow in the Strait. Next, the focus of our model study is investigation of mechanisms of pseudo–fortnightly current enhancement where passage–flow interacts with diurnal current variations, resulting in temporal change in the friction due to "form drag". Thus, we combine the study for form drag of passage–flow with the hydrodynamic interactions of diurnal tidal currents to provide some insight into the locally generated fortnightly tidal forcing within the Strait.

Key words : Tsugaru Strait, pseudo–fortnightly tide, diurnal tides, passage–flow, form drag

Introduction

Long–period lunar fortnightly (Mf) tide with 13.7–day period has much smaller amplitude than short–period semidiurnal and diurnal tides. Because of low frequency, Mf tide in the global oceans is approximately close to equilibrium, but small departure from equilibrium is also found. Such non–equilibrium response has generally been explained by the dynamics like as planetary Rossby wave or gravity wave excitations, e.g., Wunsch (1967), Miller et al. (1993) and Kantha et al. (1998). Mf tide is insignificant to overall tidal energetic, but is quite important to geophysics such as evaluating the contribution of Mf tide to tidal variations in the Earth's rotation rate.

Tidal potential of such long–period tide has no longitudinal dependence, and its meridional structure is characterized by a node with zero potential at ±35°16′ of midlatitude. Since this nodal line is just running at central part of the Japanese islands, we may expect that Mf tidal amplitude around the Japanese islands is enough small. However, after taking a careful look at tidal harmonic constants of Mf tide (see Fig. 1), unexpected large amplitudes are biased especially along the coast faced on the Japan/East Sea (JES).

One possible candidate for mechanism of this non–equilibrium response on JES is that the external forcing of Mf tide excites vigorous resonant basin modes, i.e., quasi–geostrophic normal modes in the closed basin. For example, consider rectangular basin $0 < x < x_0$, $0 < y < y_0$. Any set of mode (m, n) at x and y directions will satisfy closed boundary conditions and the steady state Rossby equation on the planetary β ($= 2 \times 10^{-13}$ cm^{-1} s^{-1}) plane, provided the oscillated frequency σ_{mn} equals the following eigenvalue (Pedlosky, 1979).

$$\sigma_{mn} = -\frac{\beta}{2\pi\left\{\left(m^2 / x_0^2\right)+\left(n^2 / y_0^2\right)\right\}^{1/2}} \qquad (1)$$

Eq.(1) notes that the lowest modes have the highest frequency, while smaller scale modes oscillate more slowly. JES is one of the marginal seas in the eastern Asia, and has a semi–closed basin (roughly $x_0 = y_0 =$ 1,500 km square with depth exceeding 3,000 m) and three shallow straits connecting to the East China Sea (ECS), North Pacific (NP) and Okhotsk Sea (OS). Selecting mode of $n = m$ ～4 in the basin scale of JES, we can take an approximate value of Mf frequency (～5.3×10^{-6} s^{-1}). Such higher mode has complex pattern of moving nodes separating cells of motion, whose phase propagation is always to the westward. However, the observed phases of Mf tide at coast in JES are almost uniform (Fig. 1 (b)), and never have the systematical mode structure.

Lyu and Kim (2005), using a simple analytic model that pressure difference between two straits connecting a marginal sea to an open ocean, studies temporal variations from subinertial to interannual time scales. They discovered a resonant

[1] *Completion of Master Course for Graduate School of Fisheries Sciences, Hokkaido University*
(北海道大学大学院水産科学研究院修士課程修了)
[2] *Laboratory of Marine Environmental Science, Graduate School of Fisheries Sciences, Hokkaido University*
(北海道大学大学院水産科学研究院海洋環境学分野)

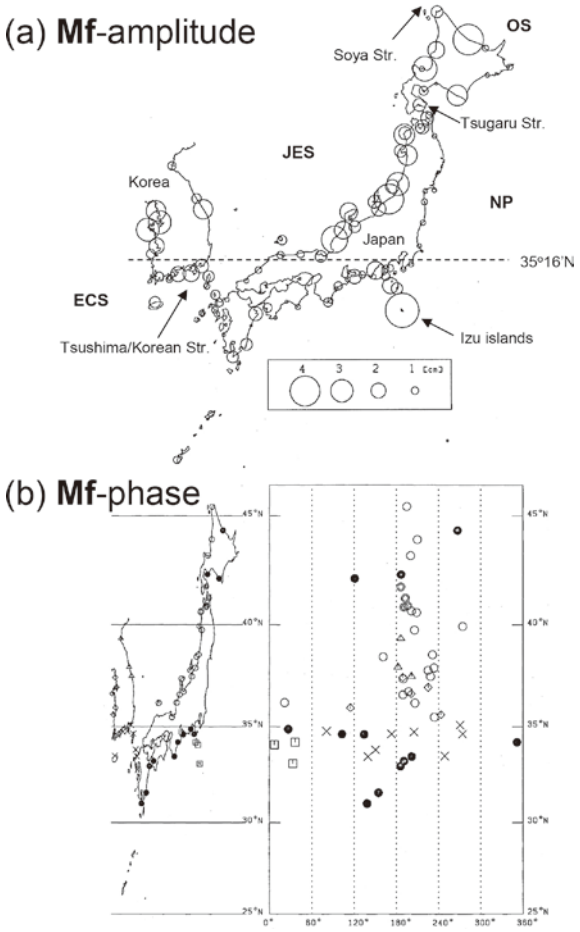

Fig. 1. Tidal harmonic constants of Mf tide at the total 104 tide-gauge stations around the Japanese islands and the Korean peninsula. (a) The amplitude is represented by a radius of circle and plotted at each station. When the amplitude of tide is less than 1 cm, the corresponding phase is not plotted because background noise is expected to be large. A nodal line along 35°16′N latitude for the long-period tidal potential is indicated by a broken line. (b) The unit of phase degree is used for phase lag referred to the local transit at the Japanese standard longitude 135°E (JSL). The phase versus latitude is shown by using the different marks at each sea area ; faced on JES (○ Japan, △ Korea), NP (●), ECS (◇), the Tsushima/Koran Strait (×), the (Tsugaru) Strait (◎), the Izu islands south of Japan (□).

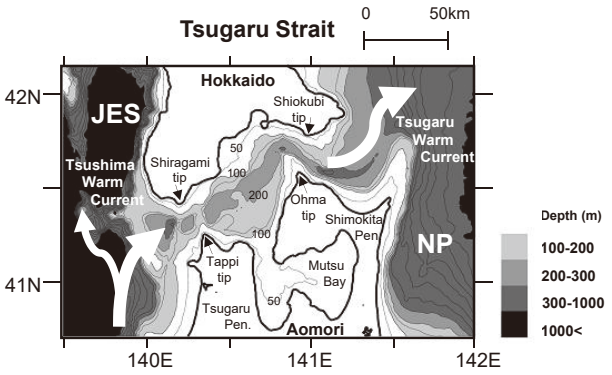

Fig. 2. The Tsugaru Strait is a narrow and shallow connecting channel between NP and JES. The dimensions of the Strait are about 100 km in length and 20～40 km in width.

frequency at which the variations of flow into and out of JES were driven by atmospheric pressure (forcing term similar to tidal potential) and mean sea level could not respond isostatically, i.e., Helmholts resonance. Its resonant period of JES is 3～5 days, which is shorter than Mf tide period. We arrived at the conclusion, at least, that quasi-geostrophic resonance or Helmholts resonance fail to explain the feature of observed deviation of Mf tide from the equilibrium.

Currents in the Tsugaru Strait (hereafter, referred to as "the Strait") are characterized by co-existence of strong diurnal tidal current and eastward passage-flow originated from the Tsushima Warm Current in JES (see Fig. 2). We combine here recent study for "form drag" of passage-flow (Iino et al., 2009) with the hydrodynamic interactions of diurnal tidal currents to provide some insight into the locally generated fortnightly tidal forcing. We elaborate on these two views as for passage-flow and tidal currents in the following paragraph.

Longitudinal axis of the Strait bends off the Ohma/Shiokubi tips near the eastern exit and the bottom geometry has several sill-topographies (Fig. 2). Iino et al. (2009) suggested that dynamic part of steady state passage flow could be understood as "form drag" caused by partial reflection phenomena, which are excited by gravitational waves over the sill-topographies. Semidiurnal tides are larger than diurnal ones in the Strait, but diurnal tidal currents in the Strait are especially enhanced (Odamaki, 1984). Both of semidiurnal and diurnal tides are almost standing waves and they are understood with a composite of the incident waves entering from both sides of the Strait (Ogura, 1932). Semidiurnal tide is in-phase in the entire Strait so that tidal current is relatively weak. For diurnal tide, a node like as amphidromic point is located near the western entrance, and hence diurnal tidal current is most dominant. Total of tidal currents and passage-flow up to about 8 knots frequently occur. These large currents cause mixing of water column through the Strait and almost homogeneous vertical structure of temperature and salinity can be formed during the tropical tides even in the stratified season (Matsuura et al., 2007).

Nonlinear interaction of dominant diurnal constituents K1 and O1 results in new oscillation with period at the fortnightly tide (13.7-day period). Therefore, we call this periodicity "pseudo-fortnightly variation" or "pseudo-Mf tide". In the present study, tides combining with passage-flow through the Strait are numerically simulated with a two-dimensional form of hydrodynamic model. Analysis of computed sea level and currents is aimed primarily at describing the enhanced currents and patterns of energy flow in the Strait. The focus of this study is investigation of mechanisms of pseudo-fort-

nightly current enhancement where passage-flow interacts with diurnal current variations, resulting in the temporal change in the friction due to form drag.

Mf tide around the Japanese islands and pseudo-Mf tidal current in the Strait

A major part of tidal harmonic constants data (Fig. 1) were taken from the Japan Maritime Safety Agency (1983) and the Korean data were quoted from tide tables of Lee (1992). In spite of small tidal potential close to nodal line of 35°16′N (less than 0.5 cm), Mf tide is more energetic along the coast faced on JES and ECS with 1～3 cm amplitude. Their phases (○◎△◇) are roughly uniform between 180° and 240°, except for the phases around the Tsushima/Korea Strait (×) and along the coast faced on NP (●□). Such distributions suggest well-organized spatial structure of Mf tide in the marginal seas. In contrast, the amplitudes in NP are much smaller less than 1 cm, except for a local area around the Izu islands. In addition, all amplitudes for monthly (Mm) tide are extremely smaller and their phases are scatted as compared to those for Mf tide (not shown). Thus, the amplitude for Mf tide are systematically too large in the marginal seas, but generally small in NP. Therefore, the difference of amplitude between both sides of the (Tsugaru) Strait is about a factor of 3～4, and the occurrence of fortnightly current variation within the Strait can be expected.

Shikama (1994) and Ito et al. (2003) reported that mean transport of passage-flow through the Strait was about 1.5 Sv by the observation for Acoustic Doppler Current Profile (ADCP). Although both studies did not give any explanation for sub-tidal variations, their time series of currents clearly indicate a significant fortnightly variation with the amplitude of 0.4～0.6 Sv or 20～40 cm s^{-1}. Tanno et al. (2005) carried out an analysis of a 13-month current data series from the mooring station near the eastern exit of the Strait and showed that periodicity of fortnightly variation was just 13.7-day (Mf tide period) for a statistical significance. Onish et al. (2004) first pointed out the existence of dominant fortnightly oscillation in the Strait by using useful ADCP data. They suggested that such fortnightly variation might be caused by large difference in Mf tide amplitude between both sides of the Strait. The present study, however, insists upon reversing the "relation between cause and result" of Onishi's suggestion. That is, the dominant part of Mf tide in the marginal seas is caused by pseudo-fortnightly variations locally generated within the Strait.

Two-dimensional model experiments

Model description

Two-dimensional form of POM (Blumberg and Mellor, 1987) is based on vertically integrated equations of motion and continuity, which are defined as follows :

$$\frac{\partial uh}{\partial t}+\frac{\partial u^2h}{\partial x}+\frac{\partial uvh}{\partial y}-fvh+gh\frac{\partial \eta}{\partial x}-F_x-Frc_x=0 \quad (2a)$$

$$\frac{\partial vh}{\partial t}+\frac{\partial uvh}{\partial x}+\frac{\partial v^2h}{\partial y}+fuh+gh\frac{\partial \eta}{\partial y}-F_y-Frc_y=0 \quad (2b)$$

$$\frac{\partial \eta}{\partial t}+\frac{\partial uh}{\partial x}+\frac{\partial vh}{\partial y}=0 \quad (2c)$$

where t is time, u and v are the vertically averaged horizontal velocity components in the x and y directions, η is the height of water surface above the mean sea level, h is the depth, f (= 9.3×10^{-5} s^{-1}) is a constant Coriolis parameter, g (= 9.8 m s^{-2}) is the acceleration of gravity. The horizontal viscosity term $F_{x,y}$ are defined as

$$F_x=\frac{\partial}{\partial x}\left[2hA_M\frac{\partial u}{\partial x}\right]+\frac{\partial}{\partial y}\left[hA_M\left(\frac{\partial u}{\partial y}+\frac{\partial v}{\partial x}\right)\right] \quad (3a)$$

$$F_y=\frac{\partial}{\partial x}\left[2hA_M\frac{\partial v}{\partial y}\right]+\frac{\partial}{\partial y}\left[hA_M\left(\frac{\partial u}{\partial y}+\frac{\partial v}{\partial x}\right)\right] \quad (3b)$$

where A_M, the vertically integrated horizontal eddy viscosity, is defined by the Smagorinsky formulation

$$A_M=C\Delta x\Delta y\frac{1}{2}\left|\nabla U+(U)^T\right| \quad (4)$$

where C (HORCON parameter) was set to be 0.1, Δx and Δy are grid spacing in the x and y directions, and $U=(u,v)$ is current vector. The bottom friction was assumed to be represented by a quadratic term with coefficient C_d (= 0.0025),

$$Frc_x=C_du\sqrt{u^2+v^2} \quad (5a)$$

$$Frc_y=C_dv\sqrt{u^2+v^2} \quad (5b)$$

Locations of open boundary are marked by dashed lines, and then the northern and southern boundaries marked by thick solid lines are artificially closed (see Fig. 3). The maximum depth is limited to 1,000 m, because the targeted area is the shallow Strait. The barotropic water motion is derived from tidal elevation which is represented by four major tidal constituents, M2, S2, K1 and O1. These are given along the east and west open boundaries by sea level oscillations, but tide-generating force around the Strait is neglected. The passage-flow from JES to NP is also produced by the fixed mean values of sea level difference $\Delta\eta$ between both open boundaries. Temporal mean volume transport through the Strait in the present model becomes close to 1.5 Sv when $\Delta\eta$ = 16 cm, i.e., the mean values were set to be +16 cm and 0 cm along the west and east open boundaries, respectively. This difference of $\Delta\eta$ will be reasonable because the observed annual mean coastal sea level difference between

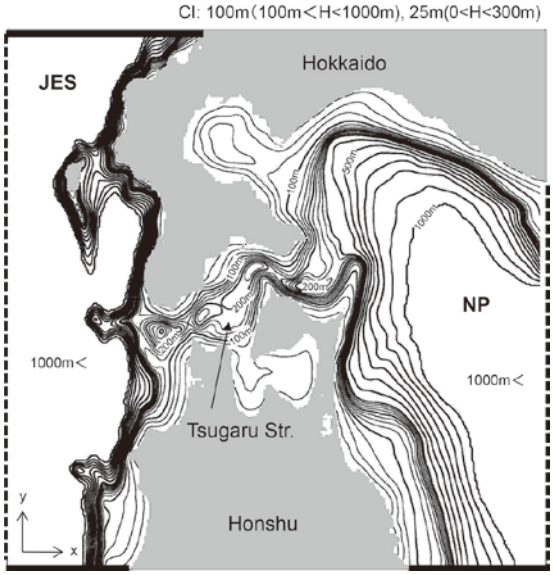

Fig. 3. Model domain, including not only the Tsugaru Strait but also part of JES (west) and NP (east). The grid bottom topography somewhat smoothed to avoid the numerical divergence, which is apt to occur around some sill-topographies in the Strait due to large diurnal tidal currents.

both sides of the Strait is 15～20 cm (Isoda and Yamaoka, 1991).

The mixed tide (four constituents) was computed for a one-month period. During the first half month, when total energy of the system become stationary. So, the standard for tidal harmonic analysis (Mf in addition to the forcing constituents of M2, S2, K1, and O1, so five constituents in all) is a last half-month-long series with one-hour sampling.

Validation of computed tides in the Strait

The similarity between the estimated and computed charts for M2 and K1 tide suggests to accuracy of the model results (Fig. 4). For M2 tide, the amplitudes are larger in NP and gradually decrease to JES through the Strait, and the phases are almost uniform within the limit of about 10°. For K1 tide, the amplitudes at western entrance of the Strait are locally small due to the formation of a southward shifted amphidromic point. In the model case without passage-flow (not shown), one amphidromic point for diurnal tides was clearly formed at the just center across the western entrance of the Strait. Isoda and Baba (1998) showed that the secondary flow produced by nonlinear interaction between strong diurnal currents and passage-flow changes in diurnal current phase due to standing waves, so that the location of amphidromic point is remarkably shifted to further south.

Residual current and its fortnightly cycle in the Strait

To extract time-averaged residual motion, the computed currents were averaged over a 15-day period, and the results of this averaging are shown in Fig. 5 (a). The eastward flow dominates in the model case with passage-flow ($\Delta\eta = 16$ cm), while the tidal residual circulations are found in the narrow some parts of the Strait in the model case without passage-flow ($\Delta\eta = 0$ cm). It has been known that such tidal

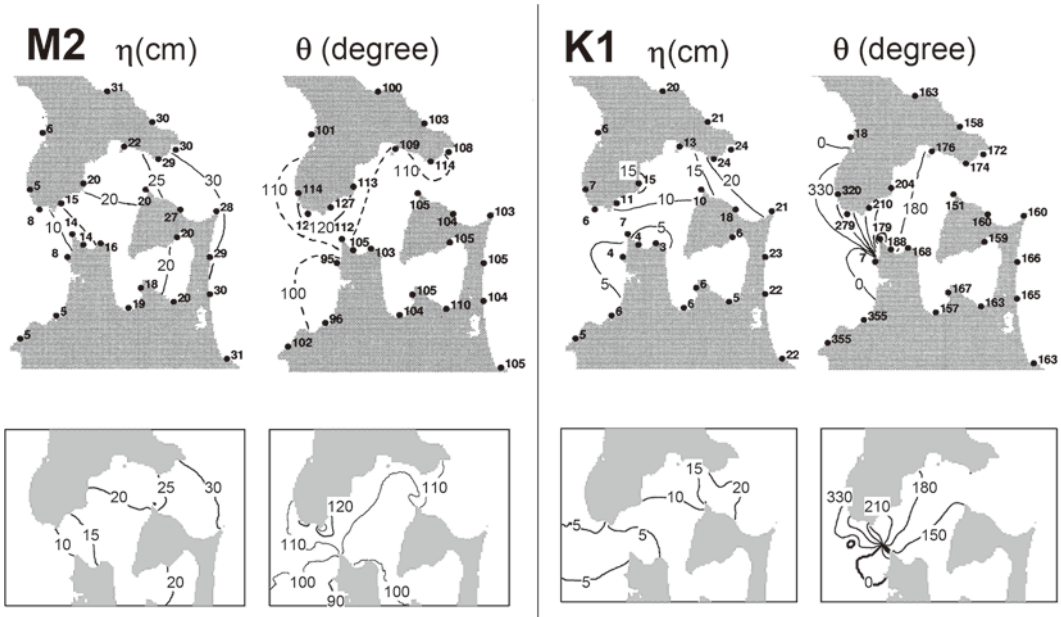

Fig. 4. In the model case with passage-flow, co-amplitudes (η in cm) and co-phases (θ in degree ; JSL) charts that we obtained of tidal elevations for M2 and K1 constituents (lower panels), together with those estimated from tidal harmonic constants based on the coastal tide-gauge stations (upper panels). S2 and O1 constituent charts (not shown) generally repeat the patterns of M2 and K1 constituents, respectively. The results in the model case without passage-flow were almost similar to ones shown in these figures except for small discrepancy of co-phase chart for diurnal tide (see text).

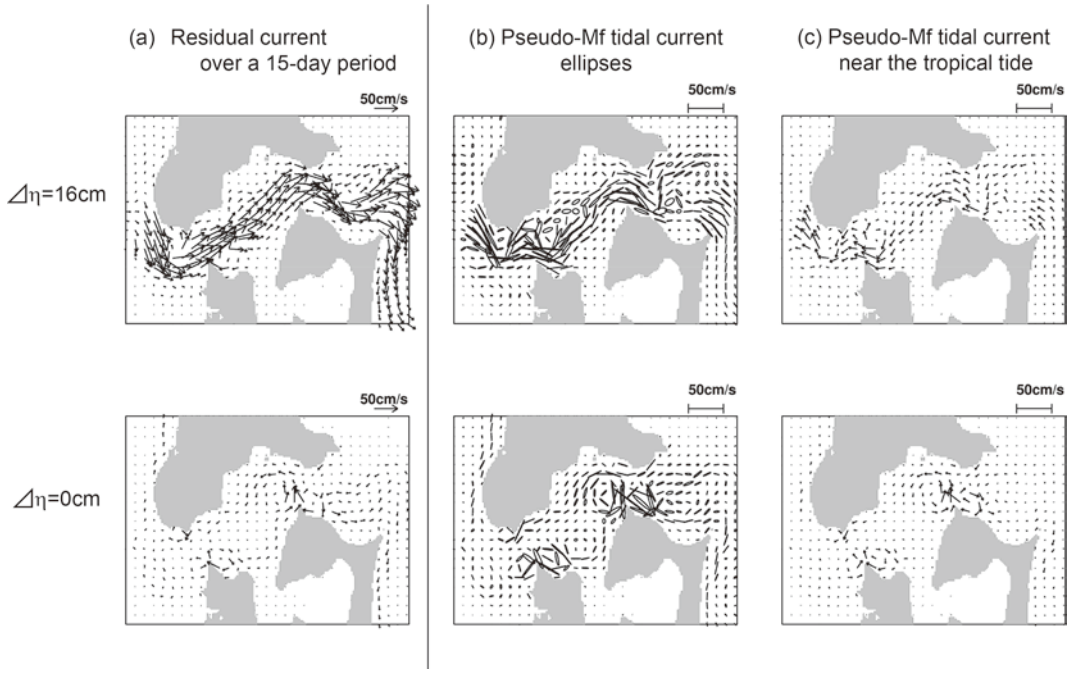

Fig. 5. (a) Residual current vectors averaged over a 15-day period, (b) current ellipses for pseudo-Mf tide component, and (c) pseudo-Mf tidal current vectors near the tropical tide, in the model cases with passage-flow of $\Delta\eta = 16$ cm (upper panels) and without passage-flow of $\Delta\eta = 0$ cm (lower panels).

residual circulations are generated by nonlinear interactions due to variable bathymetry, e.g., Zimmerman (1978), Yanagi (1976) and Yanagi (1978).

Time-dependent fluctuations of residual current (or tidal residual current) are dominated by a fortnightly cycle. None of low frequency constituents is included in the forcing. Thus, in this region, they arise through interaction between diurnal constituents (K1 and O1), which are used to force the model. The results indicate that tide having a 13.7-day period (pseudo-Mf tide period) is dominant components in the Strait. Figure 5 (b) shows the spatial structure of current ellipses for pseudo-Mf tide component as obtained from harmonic analyses of last half-month time series (i.e., about 1-cycle data) for the model cases with and without passage-flow. We refer to the largest diurnal tides as "tropical tides" as opposed to the lowest diurnal tides that we refer to as "equinoctial tides". Figure 5 (c) displays the flow patterns near the tropical tides for both model cases. In the common property of both cases, the major axes for pseudo-Mf tidal ellipses are significantly larger than the minor ones, and their orientations almost correspond to the directions of residual currents. That is, pseudo-Mf tidal currents indicate strength and weakness of residual current velocity. In the model case without passage-flow, pseudo-Mf tidal currents at the tropical tide (lower in Fig. 5 (c)) have almost the same flow pattern of residual current (lower in Fig. 5 (a)). This implies that the residual currents at the tropical tide are stronger than those at the equinoctial tide. Although such tidal residual currents play an important role in the local mean circulations, they can never contribute to net transport through the Strait. On the other hand, the model results with passage-flow (upper panels in Fig. 5) show that eastward transport through the Strait decreases at the tropical tide. It seems that tidal residual currents may not be seen like as the closed circulations because of masking by strong passage-flow. Hereafter, we focus on

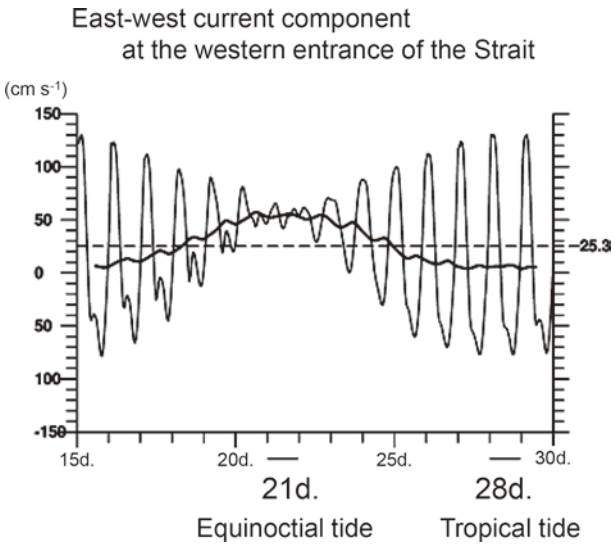

Fig. 6. Time series of east-west current component during a last-half month (15-30 day) at a grid point where the maximum velocity appears near the western entrance in the Strait. Thin and thick lines denote the 1-hour interval velocity and the residual velocity taken by 25-hour running mean filter, respectively.

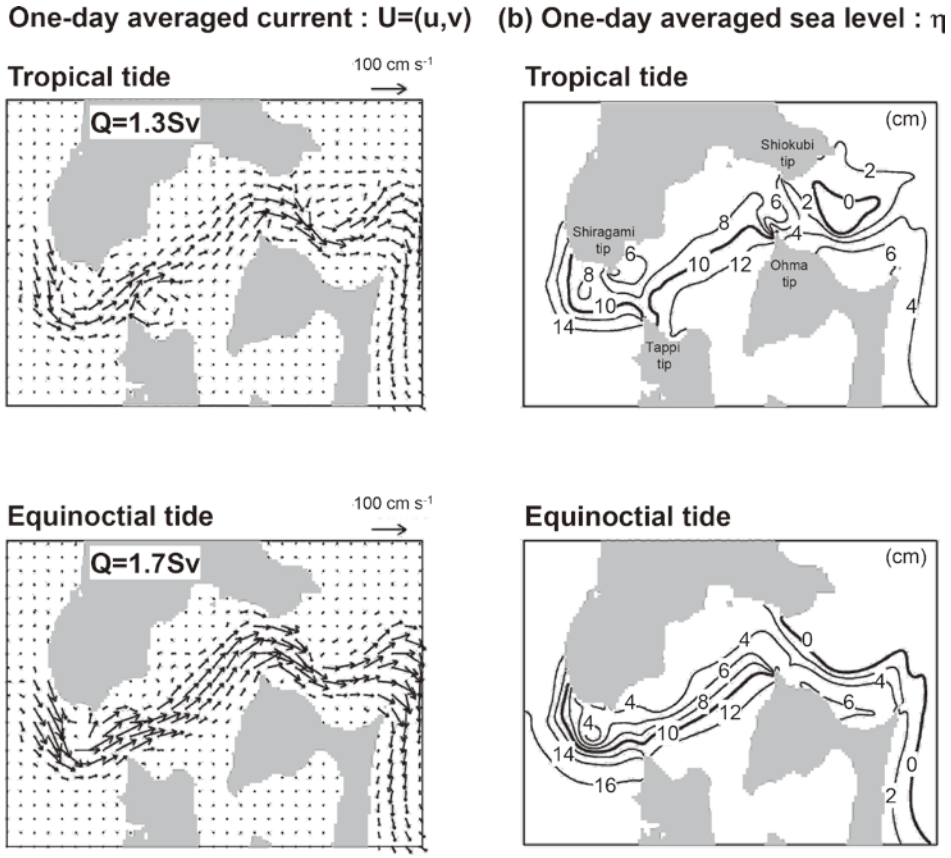

Fig. 7. One-day averaged (a) current vectors and (b) elevations for the tropical tide (upper panels) and the equinoctial tide (lower panels). An eastward passage-flow through the Strait at the equinoctial tide (volume transport is Q = 1.7 Sv) is stronger than that at the tropical tide (Q = 1.3 Sv).

this large variation of passage-flow (eastward transport) with pseudo-Mf periodicity.

Figure 6 shows, as an example, time series of east-west current component during a last-half month at a grid point where the maximum velocity appears near the western entrance in the Strait. The tropical tide is mainly characterized by periodical flow with one-day cycle, i.e., dominant diurnal tidal current. It seems that the fortnightly residual flow directly responds to temporal change in the magnitude of diurnal tidal currents. So, based on this figure, we chosen two calculate dates of 21 and 28 day as the representation for equinoctial and the tropical tides, respectively.

One-day averaged currents and elevations for each tide are shown in Fig. 7 (a) and (b). Common relationship between currents and elevations in both tides is as follows. In the central part of the Strait, the sea level contours associated with passage-flow would run along the Strait axis, suggesting "geostrophically controlled" flow. In two narrow parts of the Strait (i.e., Shiragami-Tappi tips and Shiokubi-Ohma tips), however, sea level would be locally reduced in the down-stream direction of passage-flow, suggesting like as "frictional controlled" flow. Therefore, substantial sea level difference between JES and NP occurs at these narrow areas.

Since our model is forced by imposing a mean sea level difference ($\Delta\eta$ =16 cm) between two basins at the open boundaries, the calculated sea level variation due to difference of passage-transport may be distorted by these boundary conditions. Then, we estimated a possible amplitude η_{Mf} for pseudo-Mf tide (period is T = 13.7 day) in JES basin side due to the different volume transport of eastward passage-flow (ΔQ = 1.7 − 1.3 = 0.4 Sv) using the following equation.

$$\eta_{Mf} = \frac{(\Delta Q/2)\int_0^{T/2} \sin\left(\frac{2\pi}{T}t\right)dt}{A} = \frac{\Delta QT}{2\pi A} \qquad (6)$$

where A (= 1.0×10^6 or 2.25×10^6 km^2) is the total sea surface area for JES or JES+ECS. Assuming that sea area of JES or JES+ECS is completely closed, the estimated amplitude given by eq.(6) is the order of 3.4～7.5 cm. If gravity waves originated from the (Tsugaru) Strait can rapidly propagate into the whole basins, this estimated value will be well worth explaining the observed Mf tide with amplitude of 1～3 cm and almost same phase in JES and ECS.

Energy flux and dissipation of passage-flow

In the presence of boundary forcing, sea level at open boundaries is adjusted so as to keep the difference. Therefore, some adjusted process within the Strait must occur with

the time scale of pseudo-Mf tide period to strengthen and weaken passage-flow. So, volume transport through the Strait should be determined by the dynamics in the Strait. Our model results demonstrate that damping of sea level becomes significant at the local two areas. Therefore, part of volume transport should be frictionally controlled. At first, the passage-flow state is examined by considering energy flux for dissipation.

Energy flux (EF) per unit length for passage-flow (e.g., Kowalik and Proshutinsky, 1993) is given by

$$EF = (h+\eta)\rho_0\left(\frac{U^2}{2} + g\eta\right)U \qquad (7)$$

where h is the water depth, η is the elevation, ρ_0 is representative seawater density (= 1,026 kg m^{-3}), U is the current velocity for passage-flow, and g is the acceleration due to gravity.

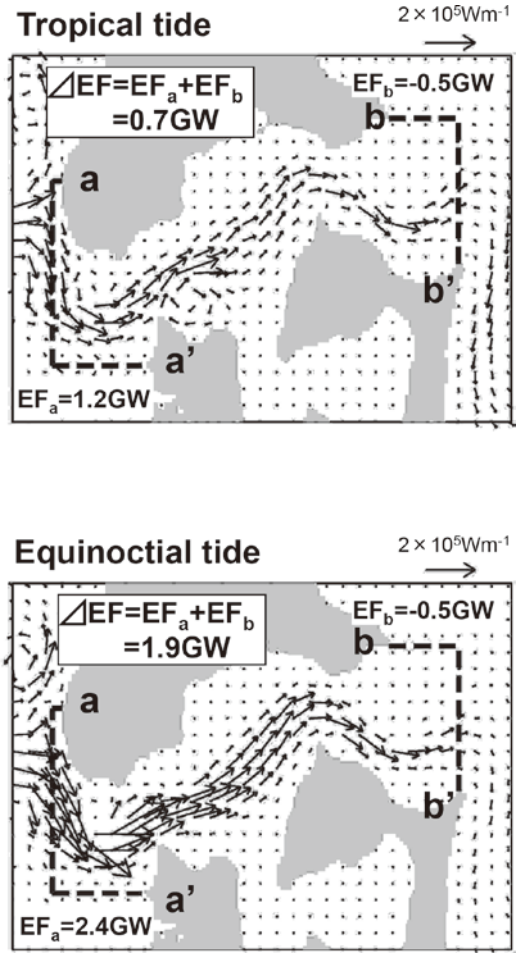

Fig. 8. Spatial distributions of energy fluxes for passage-flow at the tropical tide (upper) and the equinoctial tide (lower). Power fluxes of passage-flow normal to two transects (EF_a and EF_b), located at the western (a-a′) and eastern (b-b′) mouths of the Strait, are net fluxes into the Strait being positively defined and the fluxes out of the Strait being negatively defined ; EF_a = +1.2 GW and EF_b = −0.5 GW for the tropical tide, EF_a = +2.4 GW and EF_b = −0.5 GW for the equinoctial tide.

Average energy fluxes for passage-flow at tropical and equinoctial tides were computed using elevation and current at a given grid point displayed in Fig. 8. These tropical and equinoctial fluxes, which give estimates for the minimum and maximum of the barotropic fluxes with passage-flow, clearly indicate that source of energy is the advective flux from JES into the Strait. Since outgoing fluxes (EF_b) in both tides are comparable and small, almost energy is dissipated within the Strait. Such energy dissipation can be estimated as the sum of both fluxes at two sections, i.e., $\Delta EF = EF_a + EF_b$. For the tropical and equinoctial tides, the dissipation within the Strait is 0.7 GW and 1.9 GW, respectively. The dissipation at the tropical tide is less than half of that at the equinoctial tide.

One candidate for dissipation mechanism would be energy loss due to bottom friction (BF). A rate of this energy dissipation is defined as

$$BF = \frac{1}{T}\int_0^T C_d\rho_0\left(u(t)^2 + v(t)^2\right)^{3/2} dt \qquad (8)$$

where C_d is the bottom drag coefficient, ρ_0 is the seawater density, $u(t)$, $v(t)$ are the temporal change in velocity components at a given grid point, and T is the diurnal tidal period (25 hours). The currents, required for the flux time series computations, were the sum of tidal currents and passage-flow

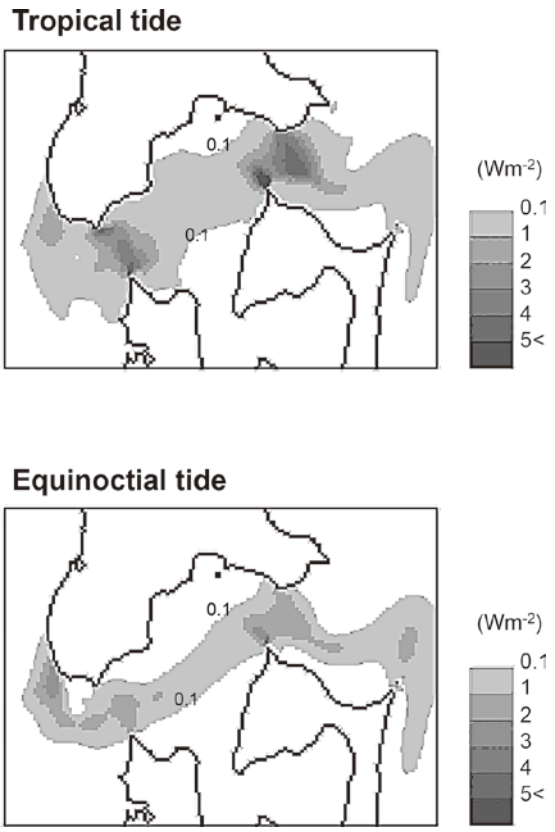

Fig. 9. Spatial distributions of bottom friction (BF) rate at the tropical tide (upper) and the equinoctial tide (lower). This dissipation process is not uniform in the Strait.

using a time interval of 1 hour. Figure 9 displays spatial distribution of this rate at the tropical and equinoctial tides. Their maximum rates are generally found in the two narrow parts of the Strait, i.e., in the region with the maximum tidal current velocities (not shown). In this region of the maximum dissipation, the rate at the tropical tide (more than 5 W m^{-2}) is greater than double of that at the equinoctial tide (~2 W m^{-2}), and hence such large and small relationship for dissipation due to bottom friction is opposite sense of the dissipation for passage-flow.

Theoretical consideration for a linear frictional coefficient rearranged from the effect of form drag

We newly propose another candidate for the dissipation mechanism of passage-flow, which is related to form drag in the Strait. It is found that passage-flow gets through several sill-topographies with large amplitude more than 100 m in Fig. 10 (b). Iino et al. (2009) carried out the similar model simulation with no tidal forcing, whose case corresponds to the equinoctial tide in our calculation. They pointed out that steady passage-flow was given after partial reflection phenomena due to the genesis of gravitational waves over sill-topography, i.e., form drag mainly contributed to the

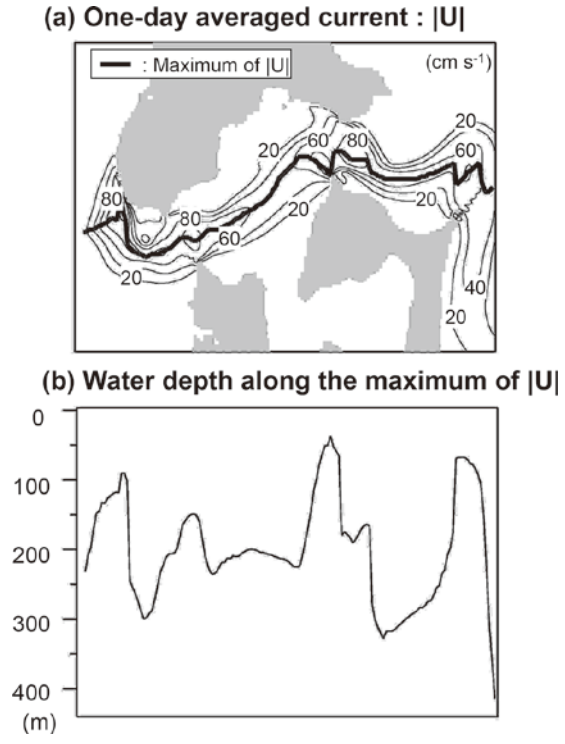

Fig. 10. (a) Spatial distribution of absolute value |U| of one-day averaged current at the equinoctial tide (lower in Fig. 7 (a)), and thick solid line indicates the flow-axis (i.e., the maximum value line of |U|) of calculated passage-flow. The qualitative similar pattern holds true for the tropical tide considered (not shown). (b) Horizontal (east-west) distribution of bottom topography along this flow-axis.

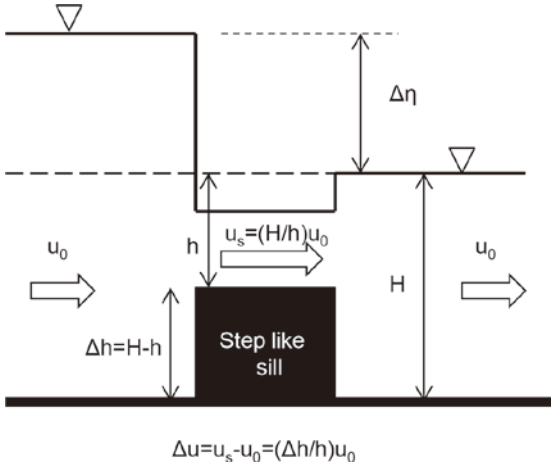

Fig. 11. One-dimensional channel model for the step like sill-topography (Iino et al., 2009). When sill-depth is h (< H ; channel depth), $\Delta\eta$ is net sea level difference due to form drag, u_0 is velocity of passage-flow, Δu is the shear flow before and after sill-topography.

dynamics for passage-flow.

Furthermore, Iino et al. (2009) found a simple relationship between net sea level difference ($\Delta\eta$) due to form drag and the down-stream shear flow (Δu) before and after a step like sill-topography ($\Delta h / h$), using the idealized one-dimensional channel model (we defined variables as indicated in Fig. 11) as follows ;

$$\Delta\eta \propto (\Delta u)^2 = \left(\frac{\Delta h}{h} u_0\right)^2 \qquad (9).$$

Based on this relationship, let us consider the response of sea level difference for the periodic changes in the current within the Strait. The velocity is expressed as the sum

$$u_0 = u_c + u_a \sin(\omega t) \qquad (10)$$

where u_c is a constant passage-flow velocity and u_a is the amplitude of diurnal tidal velocity (ω is the diurnal frequency). Integration over the one period ($2\pi / \omega$) and use of eqs.(9) and (10) gives

$$\Delta\eta \propto \left(\frac{\Delta h}{h}\right)^2 \left(u_c^2 + u_a^2\right) = r^*(u_a) u_c \qquad (11)$$

where

$$r^*(u_a) = \left(\frac{\Delta h}{h}\right)^2 \left(u_c + \frac{u_a^2}{u_c}\right) \qquad (12)$$

is a linear frictional coefficient rearranged from the effect of form drag for function of u_c and u_a. Needless to say, if $\Delta h \to 0$ (no step-like sill), $\Delta\eta \to 0$ (there is no effect of form drag). Refereeing to the example for velocity shown in Fig. 6, tidal amplitude (u_a) becomes 0 cm s^{-1} at the equinoctial tide and reaches 100 cm s^{-1} at the tropical tide. Since this maximum value of u_a is generally the same order or greater than that of u_c in the study area, eq.(12) denotes that the value

of $r^*(u_a)$ at the tropical tide is at least more than double than that at the equinoctial tide. Assuming that sea level difference of both sides of the Strait is fixed, our model result that the volume transport of passage-flow is weakened at the tropical tide can be qualitatively explained by the increase of form drag due to dominant diurnal tidal currents.

Here, we regard the temporal change in form drag as that in the above linearized frictional coefficient r^*, and examine the response of barotropic mean flow u_c through the Strait to total sea leivel difference $\Delta\eta$ between two basins at the nearly steady state because of $\partial/\partial t \ll f$ (Coriolis parameter) for pseudo-Mf periodicity. The following relationship between u_c and $\Delta\eta$ essentially corresponds to the steady version of Toulany and Garrett (1984) under a simple channel model of mean depth H, length L, and width W connecting two basins. First, sea level difference along the Strait is frictionally determined by

$$\Delta\eta_F = Lr^* u_c (gH)^{-1} \quad (13).$$

Next, the geostrophic sea level difference across the Strait is given by

$$\Delta\eta_G = fWu_c g^{-1} \quad (14).$$

Therefore, total sea level difference on the f-plane between two basins has

$$\Delta\eta = \Delta\eta_F + \Delta\eta_G = u_c g^{-1}(F+G) \quad (15a)$$

where

$$F = r^* LH^{-1} \quad (15b)$$
$$G = fW \quad (15c).$$

The ratio between F and G is regarded as a measure that determines whether flow is "frictionally controlled" or "geostrophically controlled". In this study, the parameter of $F/(F+G)$ is used to judge which flow is dominantly controlled.

As a reference to mean sea level across the Strait at the down-stream side, energy fluxes across two transects at the up-stream and down-stream sides, i.e., EF_a and EF_b, are taken by

$$EF_a = \rho_0 (H+\Delta\eta_F)\left(\frac{u_c^2}{2} + g\Delta\eta_F\right) u_c W \quad (16a)$$

$$EF_b = \rho_0 (H+0)\left(\frac{u_c^2}{2} + g\cdot 0\right) u_c W \quad (16b).$$

Note that net sea level difference along the Strait is not $\Delta\eta$, but $\Delta\eta_F$. Subtracting the two expressions ($\Delta EF = EF_a - EF_b$) and use of eqs.(13) and (15) gives total energy dissipation within the Strait as follows ;

$$\Delta EF \approx \rho_0 r^* u_c^2 LW$$
$$= \rho_0 W (gH\Delta\eta)^2 \frac{F}{(F+G)^2} \quad (17)$$

where $H + \Delta\eta_F$ in eq.(16a) is approximated by H because of $H \gg \Delta\eta_F$. Volume transport of passage-flow Q is given by

$$Q = WHu_c = \frac{WgH^2\Delta\eta}{F+G} \quad (18).$$

Figure 12(a) shows that energy dissipation ΔEF has a maximum value only when r^* is selected at the range of $F/(F+G) = 0.5$ (i.e., $F = G$). The limits of eq.(17) for $F/G \to 0$ and $G/F \to 0$, respectively, can be approximated by

$$\Delta EF \approx \rho_0 W (gH\Delta\eta)^2 \frac{F}{G^2} \propto r^* \quad (19a)$$

$$\Delta EF \approx \rho_0 W (gH\Delta\eta)^2 \frac{F-2G}{F^2} \propto \frac{1}{r^*} \quad (19b).$$

ΔEF increases in proportional to r^*, which corresponds to F, at the geostrophic control limit (eq.(19a) at $F/G \to 0$), but decreases in inverse relation to r^* at the frictionally control limit (eq.(19b) at $G/F \to 0$). That is, a maximum dissipation surely occurs somewhere between both limits, and it is just at the range of $F = G$.

We putted energy dissipations of 0.7 and 1.9 GW at the

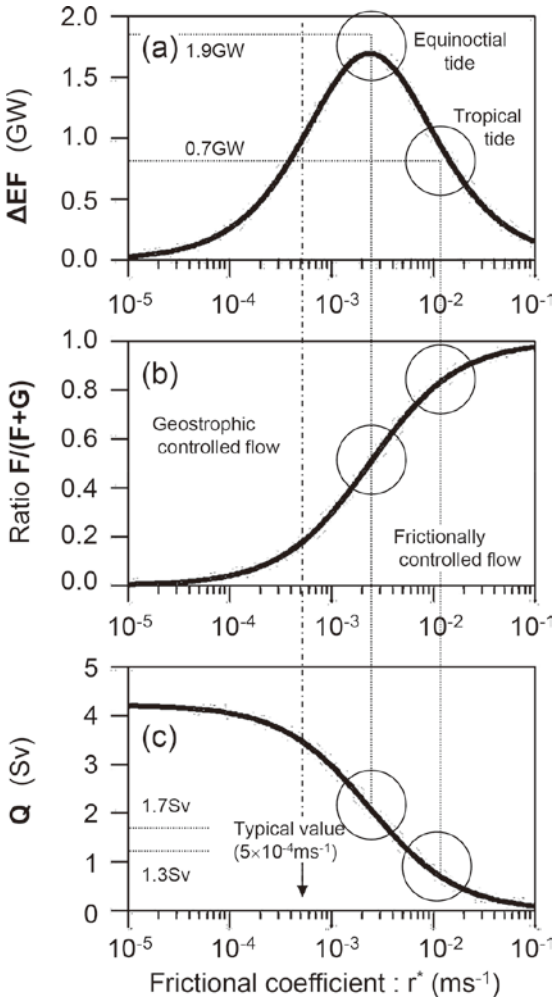

Fig. 12. Three responses of (a) ΔEF, (b) $F/(F+G)$, and (c) Q for realistic parameters of $f = 10^{-4}$ s^{-1}, $H = 150$ m, $W = 20$ km, $\Delta\eta = 15$ cm, and $L = 100$ km, where we treat as variable value for r^* in wide range from 10^{-5} to 10^{-1} m s^{-1}. When r^* increases, the frictionally controlled flow gradually dominates ($F/(F+G) \to 1$), and the volume transport monotonically decreases ($Q \to 0$).

tropical and equinoctial tides, which were given by the model results in Fig. 8, upon the responses of Fig. 12 as the symbol marks of open circle, respectively. Here, a smaller dissipation for the tropical tide was taken at the range of fictionally control (i.e., $F/(F+G) > 0.5$), because the calculated transport of passage-flow at the tropical tide ($Q = 1.3$ Sv) was smaller than that at the equinoctial tide ($Q = 1.7$ Sv). Although these values do not entirely match to the theoretical responses with a simple channel model, the flow system can be interpreted by this theory. Frictional coefficient at the equinoctial tide is $r^* \sim 2.5 \times 10^{-3}$ m s^{-1} having the nearly maximum of ΔEF (i.e., $F \sim G$), which is one order of magnitude larger than the typical value of 5×10^{-4} m s^{-1} (e.g., Chapman et al., 1986), as already suggested by Iino et al. (2009). The present study newly reveals that frictional coefficient at the tropical tide is further large value of $r^* \sim 10^{-2}$ m s^{-1}, which is about four times as large as the value at the equinoctial tide. Thus, we believe the dissipation mechanism of passage-flow due to temporal change in form drag, which depends on the tropical and equinoctial tidal cycle, i.e., pseudo-Mf tidal period.

Summary and discussion

In this paper we examine the reason why non-equilibrium response of Mf tide dominates only in the Asian marginal seas, i.e., JES and ECS. We suppose that dominant part of Mf tide in the marginal seas is caused by pseudo-fortnightly variations locally generated within the (Tsugaru) Strait. The models in this study were forced by adjusting sea levels at open boundaries so as to keep the difference in mean sea level. The dissipation mechanism of passage-flow was discussed under the fixed sea level difference along the Strait. In reverse, Iino et al. (2009) examined the response of sea level difference to varying passage-flow. Their physical interpret is as follows ; part of inflow-energy cannot pass through the Strait and is accumulated at the up-stream side as the rise of sea level. At present, the validity of both artificial forgings cannot be justified. This is ascribed to the unsolved problem of how the dissipation energy of passage-flow through the Strait is converted into the potential and kinetic energies around open oceans. Thus, to clarify this problem is indispensable for a full understanding of the current system around the Japanese islands. In the present stage, we can only propose the qualitative relationship between weakened/strengthened passage-flow and sea level rise/fall at the up-stream side of the Strait, synchronized with the period of tropical/equinoctial tide.

The present theory can be also applicable to passage-flow through the Soya Strait which is another outflow exit of the Tsushima Warm Current, because this strait has a sill topography shallower than 50 m depth and diurnal tidal current is also significantly dominant (e.g., Aota and Matsuyama, 1987 ; Odamaki, 1994 ; Ebuchi et al., 2006). Recently, Ebuchi et al. (2009) statistically analyzed the time series data for 1024 days obtained by HF (high frequency) ocean radars, bottom-mounted ADCP, and coastal tide gauges around the Soya Strait, and found a most dominant fortnightly oscillation (Mf tide) for both current (or transport) and sea level (or sea level difference) in the subinertial frequency band from 5 to 20 days. However, the coherence between these currents and sea level was very low at the Mf tide frequency. Base on this result, they suggest that it is difficult to interpret fortnightly variations using only the Mf tide amplitude difference between two seas. So, instead of Mf tide variation, they conclude that sea level difference through the strait caused by wind-generated coastal trapped shelf waves on both sides of the strait can be considered as a possible mechanism causing the subinertial variations. However, since the spectrum of wind stress does not have a peak at the Mf tide period, but around 5 days, the reason for predominance of fortnightly oscillation is still missing.

In this study we have considered a possibility for genesis of pseudo-Mf tide produced by interaction between passage-flow and dominant diurnal tidal currents through the discussion as for form drag. We think that similar physical situation is also realized in the Soya Strait, but only during a half-year with summer as the central season. This is because passage-flow through the Soya Strait has a clear seasonal variation, being stronger in summer and almost disappearing in winter (Ebuchi et al., 2006). Based on our model result in Fig. 5 for residual currents in the (Tsugaru) Strait, we readily infer that pseudo-Mf tidal currents dominate as passage-flow in summer, while in winter as tidal residual current with a closed circulation, which is presumably confined to local area around the Soya Strait. That is, residual current has the Mf-tide periodicity throughout the year, but its current direction at a specific point might be largely changed with a seasonal periodicity. If so, we understand that Ebuchi et al. (2009)'s statistical result for low correlation between current and sea level at the Mf tide period may be caused by using the long-term data without distinction of seasonality. Although such seasonality should be verified, the Soya Strait is likely another generation area for pseudo-Mf tide, at least in summer, with the corresponding pseudo-Mf tide variation at the Tsugaru Strait.

Acknowledgments

We are deeply indebted to Dr. Hiroshi Kuroda of Hokkaido National Fisheries Research Institute for his support in the numerical simulation, when one of authors (H. Matsuura) was the graduate student in Hokkaido University. We would like to thank Dr. Masayuki Noto for his drawing the original figure of Fig. 1, which motivates to put an idea for pseudo-Mf tide into practice.

References

Aota, M. and Matsuyama, M. (1987) Tidal current fluctuations in the Soya Warm Current. *J. Oceanogr. Soc. Japan*, **43**, 276-282.

Blumberg, A.F. and Mellor, G.L. (1987) A description of a three-dimensional coastal ocean circulation model. pp. 1-16, Heaps, N. (ed.), *Three-Dimensional Coastal Ocean Models*, Vol. 4, American Geophysical Union, Washington, D.C.

Chapman, D.C., Barth, J.A., Beardsley, R.C. and Fairbanks, R.G. (1986) On the continuity of mean flow between the Scotian Shelf and the Middle Atlantic Bight. *J. Phys. Oceanogr.*, **16**, 758-772.

Ebuchi, N., Fukamachi, Y., Ohshima, K.I., Shirasawa, M., Takatsuka, T., Daibo, T. and Wakatsuch, M. (2006) Observation of the Soya Warm Current using HF ocean radar. *J. Oceanogr.*, **62**(1), 47-61.

Ebuchi, N., Fukamachi, Y., Ohshima, K.I. and Wakatsuch, M. (2009) Subinertial and seasonal variations in the Soya Warm Current revealed by HF radars, coastal tide gauges, and bottom-mounted ADCP. *J. Oceanogr.*, **65**(1), 31-43.

Iino, R., Isoda, Y. and Yahaba, H. (2009) Sea level difference inducing the passage-flow through the Tsugaru Strait. *Umi to Sora*, **85**(1), 1-19. (in Japanese with English abstract)

Isoda, Y. and Yamaoka, H. (1991) Flow structure of the Tsushima Warm Current passing through the Tsushima Straits. *Bull. Coastal Oceanogr.*, **28**(2), 183-194. (in Japanese with English abstract)

Isoda, Y. and Baba, K. (1998) Tides and tidal currents in the Tsugaru Strait. *Bull. Fish. Sci. Hokkaido Univ.*, **49**(3), 117-130. (in Japanese with English abstract)

Ito, T., Togawa, O., Ohnishi, M., Isoda, Y., Nakayama, T., Shimuzu, S., Kuroda, H., Iwahashi, M. and Sato, C. (2003) Variation of velocity and volume transport of the Tsugaru Warm Current in the winter of 1999-2000. *Geophys. Res. Let.*, **30**, 11(1-4).

Japan Maritime Safety Agency (1983) *Tidal harmonic constants table around the Japan*, 742, pp. 171.

Kantha, L.H., Stewart, J.S. and Desai, S.D. (1998) Long-period lunar fortnightly and monthly ocean tides. *J. Ocenophys. Res.*, **103**(C6), 12639-12647.

Kowalik, Z. and Proshutinsky, A.Y. (1993) Diurnal tides in the Arctic Ocean. *J. Geophys. Res.*, **98**, 16449-16469.

Lee, S.W. (1992) "*Han-gug Geun-hae Hae-sang Ji* (in Korean)", Jibmoon-dang, pp. 334.

Lyu, S.J. and Kim, K. (2005) Subinertial to interannual transport variations in the Korea Strait and their possible mechanisms. *J. Geophys. Res.*, **110**, C12016.

Matsuura, H., Isoda, Y., Kuroda, H., Kuma, K., Saitoh, Y., Kobayashi, N., Aiki, T., Wagawa, T., Yabe, I. and Hoshiba, Y. (2007) Water mass modification process of the Passage-flow waters through the Tsugaru Strait. *Umi to Sora*, **83**(1), 21-35. (in Japanese with English abstract)

Miller, A.J., Luther, D.S. and Hendershott, M.C. (1993) The fortnightly and monthly tides : Resonant Rossby waves or nearly equilibrium gravity waves ? *J. Phys. Oceanogr.*, **23**, 879-897.

Odamaki, M. (1984) Tide and tidal current in Tsugaru Strait. *Bull. Coastal Oceanogr.*, **22**, 12-22. (in Japanese with English abstract)

Odamaki, M. (1994) Tides and tidal currents along the Okhotsk coast of Hokkaido. *J. Oceanogr.*, **50**, 265-279.

Ogura, S. (1932) The tides in the seas adjacent to Japan. *Bull. Hydrogr. Dep.*, **7**, 1-189.

Onishi, M., Isoda, Y., Kuroda, H., Iwahashi, M., Satoh, C., Nakayama, T., Ito, T., Iseda, K., Nishizawa, K., Shima, S. and Togawa, O. (2004) Winter Transport and Tidal Current in the Tsugaru Strait. *Bull. Fish. Sci. Hokkaido Univ.*, **55**(2), 105-119.

Pedlosky, J. (1979) *Geophysical Fluid Dynamics*. Springer-Verlag, New York, pp. 624.

Shikama, N. (1994) Current measurements in the Tsugaru Strait using bottom-mounted ADCPs. *Kaiyo Monthly*, **26**(12), 815-818. (in Japanese)

Tanno, T., Kuroda, H., Isoda, Y. and Aiki, T. (2005) Flow variations off Cape of Esan, northeast of Tsugaru Strait. *Bull. Fish. Sci. Hokkaido Univ.*, **56**(2), 33-41. (in Japanese with English abstract)

Toulany, B. and Garrett, C.J.R. (1984) Geostrophic control of fluctuating flow through strait. *J. Phys. Oceanogr.*, **14**, 649-655.

Wunsch, C. (1967) The long-period tides. *Rev. Geophys. Space Phys.*, **5**, 447-475.

Yanagi, T. (1976) Fundamental study on the tidal residual circulation I. *J. Oceanogr. Soc. Japan*, **32**, 199-208.

Yanagi, T. (1978) Fundamental study on the tidal residual circulation II. *J. Oceanogr. Soc. Japan*, **34**, 67-72.

Zimmerman, J.T.F. (1978) Dispersion by tide induced residual current vortices. pp. 207-216, Nihoul, J. (ed), *Hydrodynamics of Estuaries and Fjords*, Elsevier, Amsterdam.